Surface Femtochemistry: Associative Desorption of Hydrogen from Ru(001) Induced by Electronic Excitations†

Daniel N. Denzler,‡ Christian Frischkorn,*,§ Martin Wolf,‡,§ and Gerhard Ertl‡

Fritz-Haber-Institut der Max-Planck-Gesellschaft, Faradayweg 4-6, 14195 Berlin, Germany, and Freie Universität Berlin, Fachbereich Physik, Arnimallee 14, 14195 Berlin, Germany

Received: February 22, 2004; In Final Form: May 3, 2004

Absorption of femtosecond near-infrared laser pulses in the surface near region of Ru(001) covered with atomic hydrogen induces recombinative desorption of its molecular species. The ultrafast time scale of this surface reaction as evidenced by two-pulse correlation measurements (fwhm of ∼1 ps) together with a nonlinear dependence of the reaction yield on the absorbed laser fluence reveals an electron-mediated reaction pathway involving nonadiabatic coupling between adsorbate vibrational degrees of freedom and transient electron−hole pair excitations in the substrate. A pronounced isotope effect in the H_2 vs D_2 yield exhibits a strong fluence dependence (H_2/D_2 ratio changes from 5:1 at 120 J/m^2 to ∼20:1 at 50 J/m^2). All experimental findings can be well described within the framework of electronic friction between the substrate and adsorbate degrees of freedom, with an effective activation energy of 1.35 eV and coupling times of 180 and 360 fs for H_2 and D_2, respectively, as parameters. A pronounced coverage dependence of the desorption yield underlines that adsorbate−adsorbate interactions play a crucial role in the hydrogen recombination reaction.

Introduction

One of the major goals in chemical physics is to develop a fundamental understanding of chemical reaction dynamics. A key concept to describe the evolution from the reactants to the products relies on the existence of a Born−Oppenheimer potential energy surface (PES) and assumes that the reaction evolves electronically adiabatically on a ground (or excited) state PES.[1] Thereby nonadiabatic coupling effects between nuclear motions and electronic degrees of freedom are neglected. This concept is also frequently applied to chemical reactions on solid surfaces, e.g., in heterogeneous catalysis. However, for highly exothermic reactions on metal surfaces, there exists evidence that the Born−Oppenheimer approximation may break down and that energy is transferred to electronic excitations in the substrate (e.g., electron−hole pairs or plasmons). Well-known examples are the emission of exoelectrons or surface chemiluminescence during the oxidation of alkali metal surfaces.[2] Moreover, the excitation of hot electrons is observed during adsorption of various gases on thin metal films grown on a n-type silicon substrate by detection of chemicurrents across the Schottky barrier.[3] Further examples for nonadiabatic effects at metal surfaces include energy dissipation in vibrational relaxation[4] or dissociative adsorption.[5]

Nonadiabatic coupling between electron−hole pair excitations and nuclear (vibrational) degrees of freedom also provides a mechanism to directly stimulate reactions by femtosecond (fs) laser excitation.[6] Absorption of a fs light pulse in the metal generates a hot electron distribution, which thermalizes by ultrafast electron−electron scattering and results in a transient nonequilibrium between electron and phonon temperatures on a subpicosecond time scale.[7] Coupling of the electronic transient to adsorbate vibrational degrees of freedom will eventually lead to processes such as desorption[8] or reactions between coadsorbed species.[9] For the mechanism of surface femtochemistry, two conceptually different frameworks have been developed. One approach treats the nonadiabatic energy transfer in terms of electronic friction,[10] whereas a second scenario invokes "desorption induced by multiple electronic transitions" (DIMET).[11] In the DIMET process, hot substrate electrons transiently populate a normally unoccupied adsorbate derived affinity level, transferring the absorbate−substrate complex to an electronically excited PES. This altered charge distribution initiates nuclear motion and, after relaxation back to the electronic ground state, the system has acquired vibrational energy. At high excitation densities, additional excitation/de-excitation cycles might occur before vibrational energy relaxation takes place on the ground-state PES, thus enabling the adsorbate to accumulate sufficient energy in the relevant coordinate to overcome the reaction barrier. Experimentally, a nonlinear dependence of the reaction yield on the absorbed laser fluence is a characteristic consequence of multiple repetition of those processes.[8,11] An adsorbate-mass dependent reaction yield (further denoted as isotope effect) can also be rationalized in the DIMET picture, in which the lighter reactant will have gained more vibrational energy after relaxation back to the ground state than its heavier counterpart due to the mass-dependent acceleration on the excited potential energy surface. Note that the two pictures (friction model and DIMET) incorporate similar physical processes in a different analytic structure. The DIMET process would correspond to a strongly temperature dependent friction coefficient in the electronic friction picture. At high excitation densities (i.e., for multiple electronic transitions between the ground and excited state PES), both scenarios are physically equivalent.[10]

For microscopic-level information on elementary surface processes, the complexity of the chemical system investigated is always a limiting factor. In this regard, the recombination of two hydrogen atoms forming a molecule, which leaves the

† Part of the special issue "Gerhard Ertl Festschrift".

* Corresponding author: Fax: +49 30 838 56059. E-mail: christian.frischkorn@physik.fu-berlin.de

‡ Fritz-Haber-Institut der Max-Planck-Gesellschaft.

§ Freie Universität Berlin.

10.1021/jp049199i CCC: $27.50
Published on Web 06/25/2004

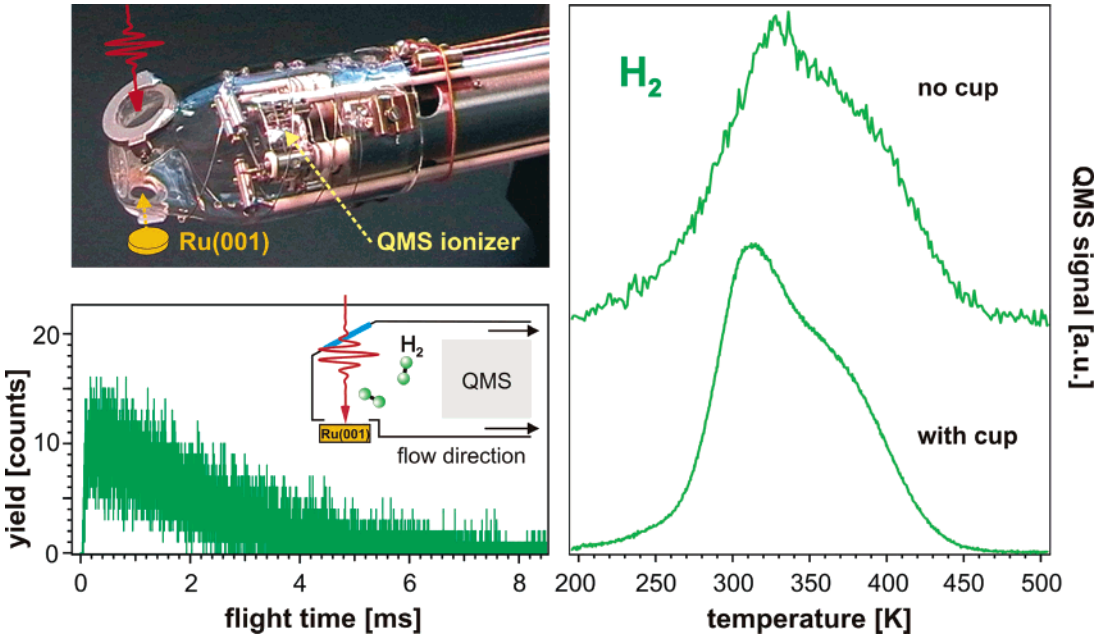

Figure 1. High-collection efficiency quadrupole mass spectrometer. Photograph of the glass enclosure around the ionizer overlaid with artwork of the incident fs laser pulse and the Ru crystal position (upper left panel) and schematical sketch of the QMS device (inset of lower left panel). The time-of-flight distribution of desorbed H_2 molecules, which for flight distances of a few centimeters typically ranges in the microsecond time scale (e.g. ~40 μs in Figure 3a), is streched in time over several milliseconds (lower left panel). TPD spectra of H_2 taken with and without the glass enclosure ["Feulner cup" according to ref 19] demonstrating the increased signal-to-noise ratio (right panel). In addition, note the different heating rates of 5 K/s and 1.5 K/s for the upper and lower spectrum, respectively.

surface, represents one of the simplest surface reactions one could think of. Hydrogen and its interaction in particular with transition-metal surfaces has attracted significant attention in both experimental and theoretical work due to its importance to technological applications such as catalytic reactions[12] and hydrogen storage in metals.[13] Fundamental research on hydrogen at surfaces has been carried out to address a variety of different aspects such as H-induced surface reconstruction,[14] substrate-mediated interaction between coadsorbed H atoms,[15,16] and quantum delocalization,[17] which might impose additional complexity of the adsorbate−substrate system despite the structural simplicity of the adsorbate.

In this article, we report on the associative desorption of hydrogen ($H_{ad} + H_{ad} \rightarrow H_{2,gas}$) on Ru(001) induced by intense fs laser pulses in the near-infrared spectral region (800 nm, 130 fs, 50−250 J/m^2 absorbed fluence $\langle F \rangle$). A brief account of this process has been given previously.[16] Here, we report detailed results on the fluence and coverage dependence of the fs laser-induced hydrogen formation. The observed mean translational energies of the desorbing molecules suggest a hot-electron-mediated process. This reaction mechanism is corroborated by two-pulse correlation (2PC) measurements of the desorption yield as well as by pronounced isotope effects in the H_2 and D_2 yields resulting from single-pulse excitations. Furthermore, the desorption yield for both isotopes increases with absorbed laser fluence $\langle F \rangle$ in a strongly nonlinear manner, as expected for multiple electronic transitions during reaction. The reaction cross section extracted out of the decay curves (yield vs laser-shot number) points to a highly efficient process in agreement with the observed saturation behavior in the fluence dependence of the yield at high fluence values $\langle F \rangle \geq 120-160$ J/m^2. Finally, we have investigated the coverage dependence of the hydrogen recombination. Our findings underline the importance of adsorbate−adsorbate interactions in the recombination process as reported in the earlier publication in which results on fs laser-induced hydrogen recombination from statistically mixed H/D layers on Ru with varying H-to-D proportions were described.[16]

Experimental Section

Experiments were carried out under ultrahigh vacuum (UHV) conditions on a single-crystal Ru(001) surface. Details of the experimental setup can be found elsewhere.[18] In short, the sample is mounted in an UHV chamber (base pressure $<1 \times 10^{-10}$ mbar) on a liquid helium cooled cryostat which in conjunction with resistive heating enables temperature control from 30 to 1530 K. Among other standard surface science tools,[18] the chamber is equipped with two quadrupole mass spectrometers (QMSs), one of them (Balzers QMS421) attached to the bottom of the chamber allowing optical access through the cross beam ionizer. In line of sight of this QMS, time-of-flight (TOF) spectra of molecules desorbed by a laser pulse can be recorded. The other QMS (Spectra Windows 200D) is mounted on a retractable translation stage aligned radially to the center of the chamber and provides a much higher collection efficiency by a home-built glass enclosure around the ionization region (so-called "Feulner cup").[19] With the sample set directly before an orifice in the enclosure, optical access is ensured by a 0.5 mm thick optical-grade fused silica window clamped to the glass body on the side opposite to the Ru crystal (left panels of Figure 1). This way, desorbing molecules undergoing multiple collisions with the inner glass walls are guided toward the QMS ionizer, however, losing angular-distribution and flight-time information. Both QMS devices can be used for temperature programmed desorption (TPD) experiments, whereby spectra taken with the high-collection efficiency QMS exhibit a significantly enhanced signal-to-noise ratio by at least one order of magnitude as compared to the signal of the convential QMS (H_2 TPD spectra in the right panel of Figure 1). Hydrogen absorbs dissociatively on Ru(001) up to saturation coverage [one monolayer (ML) H−(1 × 1)] with occupation of the three-fold fcc sites.[20] Sample preparation is carried out according to known procedures.[16,21,22] By exposing the clean Ru surface at 170 K to 50 Langmuir (1 L = 1.3 × 10^{-6} mbar·s) H_2 or D_2, saturation of either of the isotopes is achieved (1 ML). Coverages less

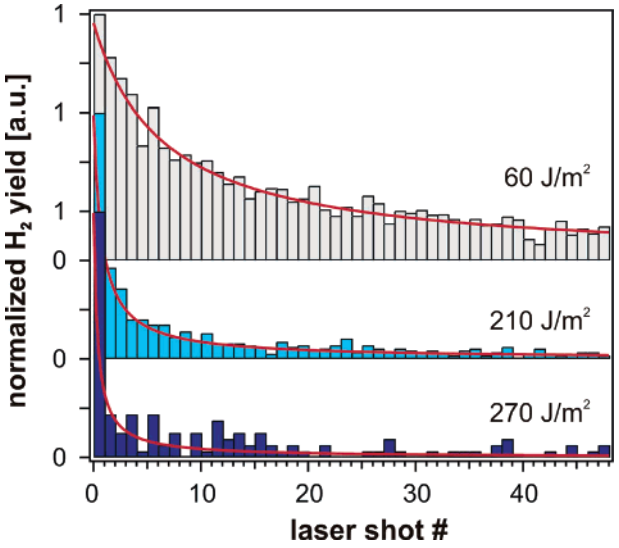

Figure 2. Decay curves of the H_2 yield from (1 × 1) coverages for various fluences ($\langle F \rangle$ = 60, 210, and 270 J/m^2) as a function of the laser shot number within a series of 50 pulses (two data sets offset for clarity). The solid lines represent fits of eq 6 to the experimental data. Note that for higher $\langle F \rangle$, the saturation coverage is almost entirely depleted within the first laser shot.

than saturation are calibrated by comparing integrated TPD yields with respect to saturation conditions.

The fs laser pulses (pulse energy up to 4.5 mJ of 130 fs duration at center wavelength of 800 nm) are delivered by a high-power laser system comprising a Ti:sapphire oscillator with regenerative and multipass amplification stages. The repetition rate can be adjusted from 400 Hz down to 20 Hz using a pulse picker between the amplification stages; single-shot experiments were performed by the additional aid of a chopper and/or shutters. The pulse energy, and hence the incident fluence, can be varied by adjusting the pump power to the multipass amplifier provided by Nd:YLF lasers. The crucial parameter for nonlinear photoinduced processes as studied here is the absorbed laser fluence $\langle F \rangle$ weighted with the respective yield (details will be given below), which enables one to compare yield data obtained with different spatial laser beam profiles. To this end, a reference beam channel is used in which the beam profile is detected by a CCD camera at a position equivalent to the Ru sample. Possible self-focusing distortions imposed by the entrance window at high laser fluences are also accounted for by placing a reference window with similar self-focusing behavior into the reference pathway.[18] Yield fluctuations caused by shot-to-shot noise can be minimized by recording a decay curve of the desorption yield as a function of laser shot number within a series of pulses impinging on the same spot on the sample. This is accomplished by detecting the desorbed hydrogen molecules with the high-collection efficiency QMS operated in a single-molecule counting mode and read out by a multichannel scaler (SRS SR430). Avoiding saturation in the detection, the recorded time-of-flight distribution is smeared out in time approximately over 2 orders of magnitude (lower left panel of Figure 1) if compared to the nascent TOF distributions shown below in Figure 3a. In a series of 50 laser shots, the time integrals of those pseudo TOF spectra (i.e., the time-strechted distributions) constitute the depletion of the coverage after multiple-pulse excitation. Figure 2 shows such decay curves for three different fluences $\langle F \rangle$ = 60, 210, and 270 J/m^2. A reciprocal power law fit (details given below, solid lines in Figure 2) to the declining yield distributions substantially reduces fluctuations in the first-shot yield (FSY).

Results and Discussion

The high density of excited substrate electrons after femtosecond-laser irradiation of the Ru substrate causes peculiar characteristics of the surface reaction which are absent in experiments using thermal excitation (i.e., under conditions of thermal equilibrium between all degrees of freedom such as

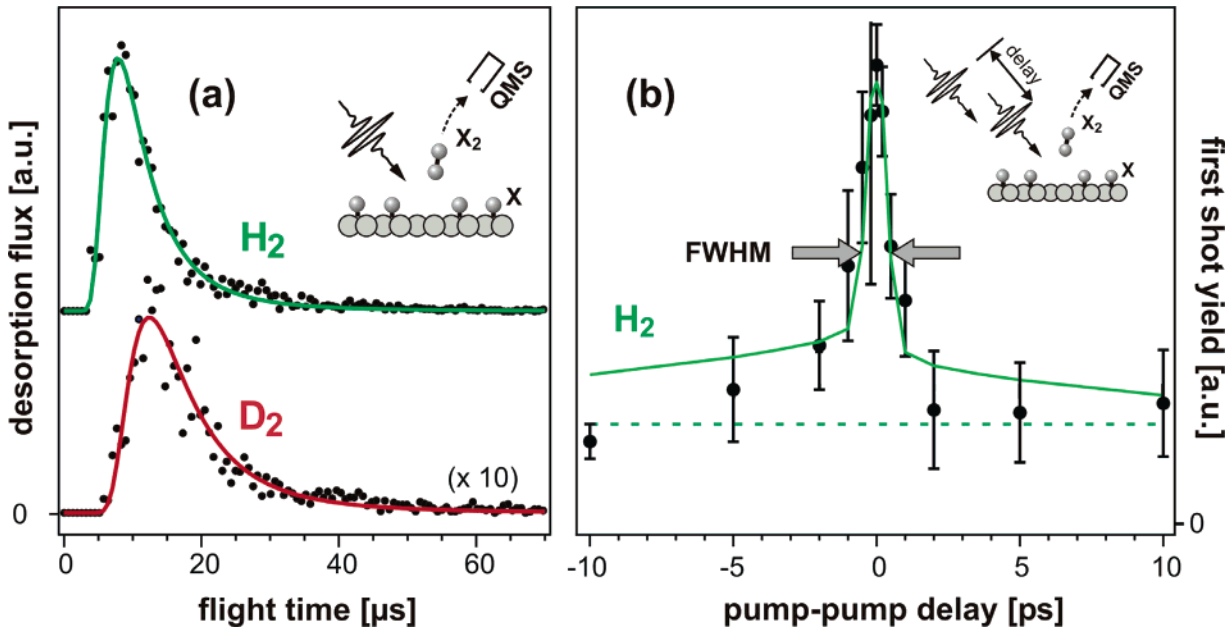

Figure 3. Femtosecond laser-induced hydrogen recombination. (a) TOF spectra of H_2 (offset) and D_2 after single pulse excitation at 60 J/m^2 absorbed fluence. Modified Maxwell−Boltzmann distributions (solid lines) fit the experimental data; the mean kinetic energies are obtained from the second momentum of the discrete experimental data points: E_{kin} = (2110 ± 400) K and (1720 ± 290) K for H_2 and D_2, respectively. The scaling factor of 10 for the D_2 data with respect to H_2 spectrum indicates the isotope effect at this particular laser fluence. (b) 2PC measurement of H_2. Here, solid lines represent the outcome of the electronic friction model [ref 10] with a coupling time τ_{el} of 180 fs and a modified activation energy E_a of 1.35 eV, resulting in a fwhm of 1.1 ps. Note that the deviation of perfectly equal pulse intensities (ratio used 54:46) causes the apparent asymmetry in the wings of the distribution.

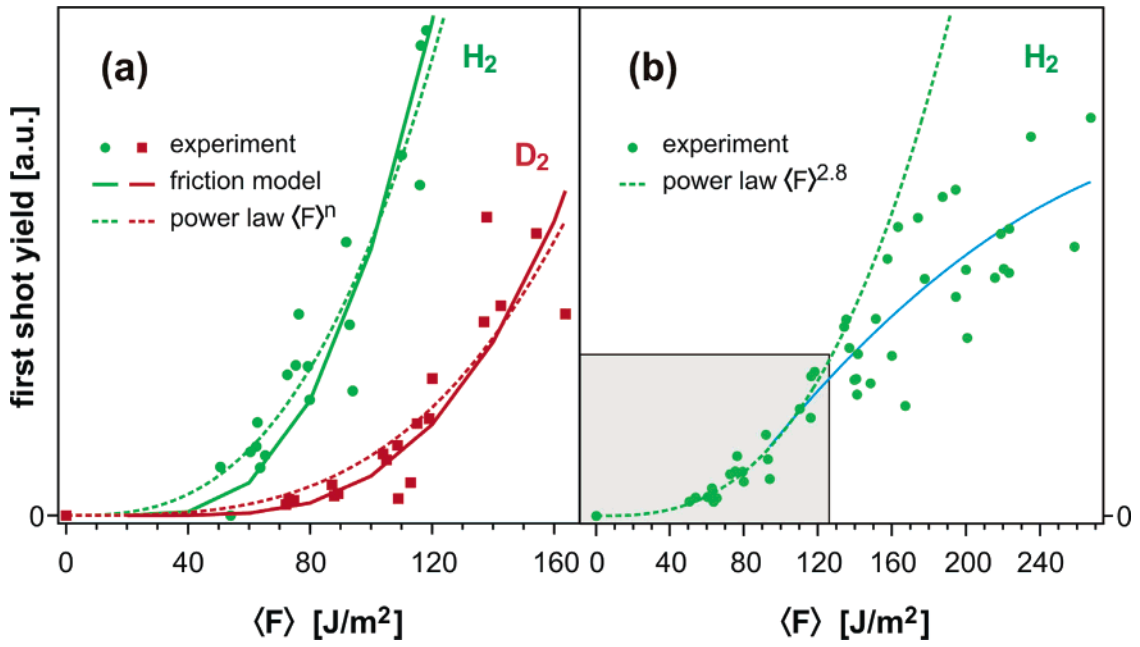

Figure 4. Fluence dependence of the H_2 and D_2 first-shot desorption yield from saturation coverage of the respective isotope. (a) First-shot yields as a function of the absorbed yield-weighted laser fluence $\langle F\rangle$, dashed lines show the parametrization by a power-law $\langle F\rangle^n$ with $n = 2.8$ and 3.2 for H_2 and D_2, respectively. Solid lines are based on the electronic friction model of ref 10 with the same coupling times and activation energy ($\tau_{el} =$ 180 and 360 fs for H_2 and D_2, respectively, $E_a = 1.35$ eV) as used for the 2PC data in Figure 3b. (b) FSY of H_2 vs $\langle F\rangle$ covering a wider fluence range from 0 to ~270 J/m^2 (near the demage threshold of the Ru crystal). Beyond 120 J/m^2 (shaded box marks the range of the left panel), the yield starts saturating as seen in the deviation from the power law $\langle F\rangle^{2.8}$ (dashed line). Solid line is guide to the eye only.

conventional resistive heating or ns-laser excitation). This is clearly reflected by the desorption dynamics. Figure 3a shows time-of-flight spectra for desorbing H_2 and D_2 molecules resulting from single pulse excitation of the Ru surface covered with a monolayer of atomic hydrogen. The mean translational temperature amounts to ~2000 K, a value much higher than for thermally induced desorption which occurs in a temperature range of 250−450 K.[21] For conditions as in Figure 3a, theoretical modeling (discussed below) predicts peak phonon temperatures below 1000 K. Consequently, a phonon-induced reaction proceeding at peak phonon temperature would result in translational energies at least by a factor of 2 smaller than observed. Higher translational energies could then only be rationalized by assuming a considerable barrier in the desorption process which, however, disagrees with the kinetics of adsorption and thermal desorption.[21] Besides the high translational temperatures from the TOF data, evidence for a hot-electron-mediated reaction mechanism is given by the ultrafast response time in two-pulse correlation (2PC) measurements of the desorption yield [see Figure 3b, full width at half-maximum (fwhm) ~1 ps]. As sketched in the inset of Figure 3b, in such a 2PC experiment, the desorption yield is measured as a function of the time delay between two equally intense pulses. A fwhm on the order of a few ps is an unambiguous fingerprint of a hot-substrate electron-driven process, whereas a phonon-mediated reaction proceeds on a much slower time scale of tens of ps.[9] The electron-mediated mechanism is corroborated by a pronounced isotope effect of 10:1 in the H_2 versus D_2 yield (at $\langle F\rangle = 60$ J/m^2, see scaling factor in Figure 3a).[16]

Still further indication is provided by the strongly nonlinear dependence of the first-shot yield (FSY) on the absorbed laser fluence as characteristic for a mechanism involving multiple electronic excitations. Figure 4 (left panel) shows the fs laser-induced FSY of H_2 and D_2 from an H and D saturation coverage, respectively, as a function of the absorbed fluence $\langle F\rangle$ exhibiting a clearly nonlinear relationship in both cases. Due to this nonlinearity, it is essential to account for the nonuniform energy distribution across the laser beam profile. For this purpose, the experimental pulse energy and spatial profile of the laser beam are recorded for each measurement. A yield-weighing procedure[18,23] is then applied in which each beam profile fraction of constant intensity is weighted with its respective yield, resulting in the absorbed yield-weighted fluence $\langle F\rangle$: by parametrization of the fluence dependence of the desorption yield Y with a power law $Y \propto \langle F\rangle^n$, $\langle F\rangle$ is obtained by summing over each camera pixel according to $\langle F\rangle = \Sigma Y_i F_i/\Sigma Y_i = \Sigma F_i^{n+1}/\Sigma F_i^n$, with n as a parameter of the self-consistent fit to the experimental data set. For both hydrogen isotopes, an exponent n of ~3 is found (2.8 and 3.2 for H_2 and D_2, respectively), shown as dashed lines in Figure 4a.

Most remarkably, comparing the absolute desorption yields per laser shot for H_2 and D_2 (experimental differences incorporated such as detection probabilities), one finds that the lighter isotope is much more readily formed by fs laser excitation than its heavier counterpart. This is in contrast to results of thermal desorption experiments where no noticecable isotope effect is found, presumably because differences in the zero-point energy are very similar in the initial and final states.[16] This isotope ratio $Y(H_2)$:$Y(D_2)$ in the fs laser experiments varies markedly with fluence $\langle F\rangle$ as shown in Figure 5; at $\langle F\rangle \sim 110-120$ J/m^2 the ratio amounts to ~5:1, whereas at low fluence a drastic increase to more than 20:1 is observed. This is consistent with the slight difference in the exponent of the parametrization of the FSY fluence dependence ($n(H_2) = 2.8$ vs $n(D_2) = 3.2$ obtained for the data in Figure 4); the D_2 formation grows faster with $\langle F\rangle$ than does the H_2 recombination, thus reducing the isotope ratio at higher fluences. One has to consider that any isotope effect should asymptotically approach unity with increasing fluence (i.e., increasing electron temperature) due to complete saturation in the photoreaction ($P_{des} = 1$) for both isotopes. However, only the high mass ratio of 2:1 in the case of the hydrogen recombination permits the observation of this

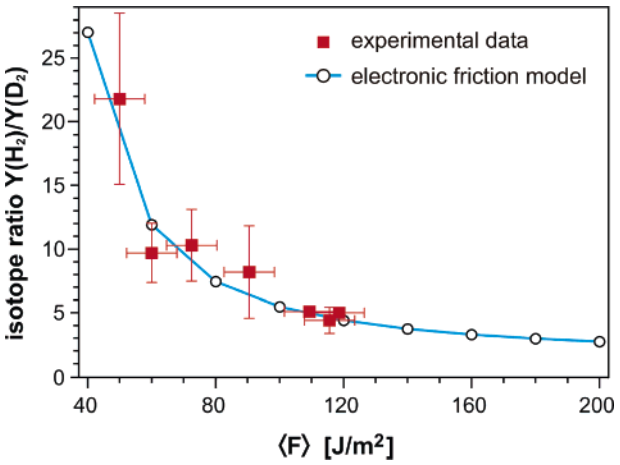

Figure 5. Isotope effect in the desorption yield $Y(H_2)/Y(D_2)$ as a function of the absorbed yield-weighted laser fluence $\langle F \rangle$. The ratio of the calculated yields for both isotopes based on the friction model (separately plotted in Figure 4) are represented by connected open symbols (○). Error bars to the experimental data points stem from multiple repetition of the measurements at similar/same fluences.

fluence dependence of the isotope effect with laser fluences below the crystal damage threshold. For example, for the CO oxidation on Ru, no such fluence dependence was observed.[9]

As becomes evident from the two-pulse correlation measurements (Figure 3b), the recombinative desorption of hydrogen from Ru(001) is mediated by hot substrate electrons.[16,22] A narrow fwhm of the 2PC on the order of 1 ps can be explained only if the electron-driven mechanism is operative.[24] For pulse−pulse separations shorter than the electron−phonon equilibration time (~1 ps for Ru), in which electron and phonon temperature T_{el} and T_{ph} are transiently out of balance, T_{el} is greatly enhanced due to the combined effect of both pulses. As a consequence of the nonlinear but complex relationship between electron temperature and reaction yield, desorption occurs predominantly during the peak temperature of T_{el}. This is reflected in the sharp rise of the hydrogen (H_2) yield vs pulse−pulse delay (as shown in Figure 3b). Note that energy transfer via the lattice phonons of the substrate proceeds on a much longer time scale (several tens of ps), thus a phonon-mediated reaction pathway would be inconsistent with the observed fast response of only 1 ps.[9,18]

To theoretically characterize the energy transfer processes initiated by fs laser excitation of a metal surface, the two-temperature model[25] (which describes the energy flow within the substrate) in conjunction with electronic friction[10,26] (which accounts for nonadiabatic coupling between the substrate and the adsorbate) is applied. In the empirical friction model by Budde et al.,[26] one describes the energy transfer from the electron and phonon system of the substrate to the adsorbate by coupling to an harmonic oscillator representing the adsorbate bath with coupling constants η_{el} and η_{ph}. Using a master equation formalism,[26,27] the time evolution of the energy content of the adsorbate is then represented by

$$\frac{d}{dt}U_{ads} = \eta_{el}(U_{el} - U_{ads}) + \eta_{ph}(U_{ph} - U_{ads}) \qquad (1)$$

with the Bose−Einstein distributed mean vibrational energy

$$U_x = \frac{h\nu_{ads}}{e^{h\nu_{ads}/(k_B T_x)} - 1} \qquad (2)$$

of an oscillator at temperature T_x. Here, ν_{ads} refers to the frequency of the vibration along the reaction coordinate. Solving eq 1 with the aid of T_{el} and T_{ph} out of the two-temperature model,[25] the adsorbate temperature T_{ads} can then be determined. Finally, the reaction rate R of an electron- and/or phonon-mediated pathway is calculated using an Arrhenius-type expression as

$$R = -\frac{d}{dt}\theta = \theta^2 k_0 e^{-E_a/(k_B T_{ads})} \qquad (3)$$

assuming second order kinetics. Alternatively, reactions induced by purely electronic friction as in the present H/Ru(001) system can also be described in a model proposed by Brandbyge et al.[10] in which Langevin noise of the electron heat bath (T_{el}) is coupled into the adsorbate system (T_{ads}) via electronic friction. Based on the same master equation as in the former case, one obtains the adsorbate temperature T_{ads} by solving

$$\frac{d}{dt}T_{ads} = \eta(T_{el} - T_{ads}) \qquad (4)$$

The reaction rate scales with the desorption probability, which in turn depends similarly to the empirical model on a Boltzmann factor

$$R(t) \propto P_{des}(t) = E_a \int_0^\infty dt \frac{\eta}{T_{ads}} e^{-E_a/(k_B T_{ads})} \qquad (5)$$

Here, however, E_a does not represent a genuine activation energy of an Arrhenius expression as in eq 3, since the friction coefficient η, T_{ads}, and E_a itself enter the preexponential factor. In a physical interpretation, E_a can be regarded as a *modified* activation energy which exceeds the depth of the desorption well, indicating the activation (i.e., population) of electronically excited states. As the reciprocal of η, τ_{el} scales inverse proportionally with the adsorbate mass and describes how fast energy between substrate and adsorbate is tranferred. Hence, the Brandbyge model directly leads to an isotope effect in the reaction yield for isotopically substituted reactants (H vs D).

Utilizing this electronic friction model by Brandbyge et al.,[10] all experimental data of the current work for H_2 and D_2 can be well reproduced: (i) the two-pulse correlation measurements, (ii) the fluence depedence of the first-shot yield, and (iii) the fluence dependence of the isotope effect. Based on a single parameter set (1.35 eV for the modified activation energy E_a and 180 (360) fs for the coupling time τ_{el} for H_2 and D_2, respectively), the solid lines in Figures 3b, 4a, and 5 are obtained. For the latter graph, the theoretical values of the isotope ratio result from division of the respective simulated H_2 and D_2 yields represented in Figure 4a.

Also shown in Figure 4 (right panel) is the fluence dependence of the first-shot yield for a wider range of absorbed yield-weighted fluences exemplarily of the desorption of H_2. For $\langle F \rangle \geq 120$ J/m^2, the experimental yields significantly deviate from the $Y \propto \langle F \rangle^{2.8}$ power law (dashed line in Figure 4b), which is used in the parametrization for smaller fluences as described above. This indicates the onset of saturation of the desorption yield ($P_{des} = 1$): parts of the H coverage are depleted during a single pulse duration. Although with increasing fluence the difference between the experimental data and $\langle F \rangle^{2.8}$ becomes more pronounced, the leveling-off of the yield is not yet completed within the fluence range applied. At fluences as high as 270 J/m^2, only the center of the laser spot on the crystal is entirely depleted, while the desorption yield from the outer regions still rises. To further quantify the efficiency of the recombination process, the reaction cross section can be extracted from decay curves of the desorption yield for multiple-

pulse excitation (see Figure 2). Assuming the number of the desorbing molecules N_i to scale proportionally with the change in coverage $\Delta\theta_i$, which for a bimolecular reaction in turn is proportional to the square of the initial coverage θ_i (before the ith laser pulse), one obtains $N_i \propto \Delta\theta_i = -\theta_i^2 f(F_i)$, with $f(F_i)$ being the general functional relationship between yield and fluence.[28] Integration yields the decay of coverage with laser shot number j according to

$$\theta_j = \frac{\theta_0}{\theta_0 \beta F_{\text{eff}}(j) + 1} \tag{6}$$

where, in the case of a nonlinear fluence dependence (as in the hydrogen recombination), $F_{\text{eff}}(j) = \Sigma_{i=1}^{j} F_i^n$ describes the effective accumulated incident laser fluence.[18,28] Here, n is the exponent of the power law parametrization given above and β a scaling constant. One can then define an effective cross section for the photoreaction by the ratio of the decay-curve exponents of the *nonlinear* (eq 6) vs the *linear* fluence dependencies and write

$$\sigma_{\text{eff}} = \beta \frac{\sum_i F_i^n}{\sum_i F_i} \tag{7}$$

With pulses of identical fluence ($F_i = F$ = const.), eq 7 simplifies to $\sigma_{\text{eff}} = \beta F^{n-1}$. For the H_2 recombination, this cross section evaluation based on fits of eq 6 to the experimental data (solid lines in Figure 2) yields $\sigma_{\text{eff}} = 6.6 \times 10^{-18}$ cm^2 at a relatively low fluence of 60 J/m^2 and rises to the 10^{-17} cm^2 range at the higher fluences. Typical cross sections for photon-induced desorption of neutrals from metals surfaces lie between 10^{-18} cm^2 and 10^{-20} cm^2.[29] For instance, a σ_{eff} of 1.7×10^{-18} cm^2 was found for the CO desorption of molecularly adsorbed species on Ru(001), however, at a high fluence $\langle F \rangle$ of 305 J/m^2.[18] If one considers that σ_{eff} depends on the laser fluence in a nonlinear fashion (see above), the cross section obtained for the recombinative desorption of H_2 indeed represents a highly efficient photoreaction. Qualitatively, this is demonstrated by the high-fluence decay curves in Figure 2 ($\langle F \rangle$ = 210 and 270 J/m^2), which decline much more rapidly compared to the desorption of CO from Ru. At 210 J/m^2 absorbed fluence, the recombination yield of H_2 drops from the first to the second laser shot by more than 60%. Yet at 270 J/m^2, almost the entire H_2 desorption of the 50-pulse sequence originates from the first laser pulse. For comparison, in the CO experiments, almost 10−20 shots at 240 J/m^2 and 305 J/m^2, respectively, were required for a similar signal reduction.

With the effective cross section, the H_2 desorption probability per pulse can be determined as $P_{\text{des}} = \sigma_{\text{eff}} F$. For an absorbed fluence of $\langle F \rangle$ = 60 J/m^2, a value of ~0.16 is obtained for P_{des} which approaches unity at the higher fluences (see above). Limitations of the validity of eq 6 include conditions in which (i) the reaction yield is coverage dependent (as will be discussed below) and (ii) surface diffusion becomes relevant. Between consecutive pulses, depleted areas of the laser-irradiated spot on the Ru crystal might be partially refilled from less depleted sections. We note, however, that all experimental decay curves of the present system can be fit by a single reciprocal power law expression of eq 6 showing no evidence of spot refilling due to surface diffusion.

That adsorbate−adsorbate interactions play a crucial role in the hydrogen recombination reaction was reported previously

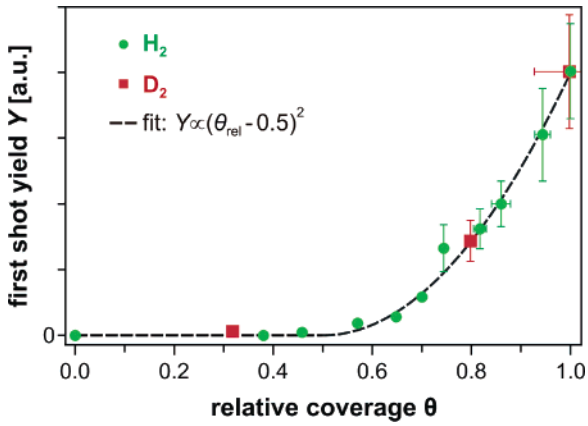

Figure 6. Coverage dependence of the fs laser-induced H_2 and D_2 desorption yield for an absorbed yield-weighted fluence $\langle F \rangle$ of ~60 J/m^2 (saturation coverage: $\theta = 1$). Relatively few data points are shown for D_2 (nomalized to the yield of H_2 at $\theta = 1$) apparently exhibiting the same $\theta - \langle F \rangle$ relationship as for the H_2 data. Note the clear threshold-like behavior that only for $\theta > 0.5$, a detectable yield is found as underlined by the dashed line (function used $Y = 0$ [0,0.5] and $(\theta - 0.5)^2$ [0.5,1]).

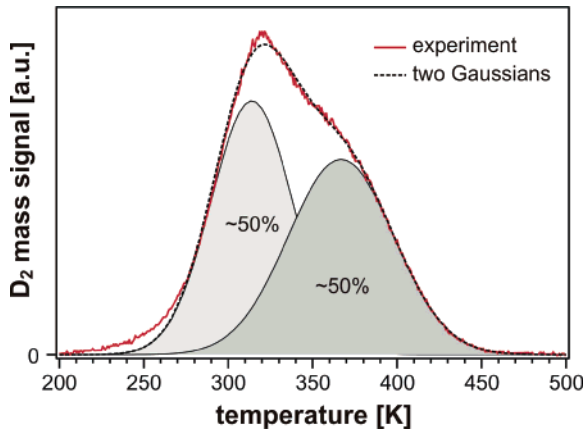

Figure 7. D_2 TPD spectrum taken at constant heating rate of 1.5 K/s with the high-collection efficiency QMS. Two maxima are located at ~320 and ~380 K and are empirically represented by two Gaussian distributions of equal integrated area. Note the TPD spectrum is well reproduced (dashed line).

in our fs laser experiments with isotope-mixed layers, in which, depending on the reactants' surrounding, a dynamic promotion effect was observed.[16] It was demonstrated that ultrafast excitation of coadsorbed H atoms enhances the reaction rate in the D_2 formation. Such effects can only be rationalized by pronounced adsorbate−adsorbate interactions, which are mediated by subtle changes of the electronic structure. This interpretation is further substantiated by the coverage dependence of the desorption yield from isotopically pure H or D layers, as shown in Figure 6. Only for coverages θ above a threshold of ~0.5 ML does the desorption yield rise above detection limit and reach its maximum at the saturation coverage of $\theta = 1$ ML. Possible origins are a coverage dependence of the binding energy and/or the electronic friction coefficient.

Inspection of the thermal desorption spectrum for 1 ML D_2 from Ru(001) (see Figure 7) provides additional insight into adsorbate−adsorbate interactions in this system. The characteristic maximum in the TPD at 320 K and the shoulder around 380 K are in accordance with earlier reports.[16,21] Unlike the initial interpretation of the TPD data, according to which the two desorption peaks originate from adsorbates on two different adsorption sites,[21] it is now commonly accepted that hydrogen

atoms on Ru occupy the 3-fold coordinated sites (fcc is energetically slighly favored against hcp by ~50 meV)[30,31] at *all* coverages[32−34] and that the shape of a hydrogen TPD spectrum is caused by increasing repulsive adsorbate−adsorbate interaction at higher coverages. The system exhibits complex thermal desorption kinetics resulting in a coverage dependent desorption order and an activation energy, which changes from 0.62 eV/atom at $\theta \approx 0$ to 0.47 eV/atom near saturation.[21] Despite this complexity, one can estimate the relative coverage at which the spectral feature at 320 K (i.e., with lower activation energy) appears in the TPD spectra. As shown in Figure 7, two Gaussians of approximately equal integrated area give a good fit to the TPD data. Apparently, for both the thermally and the fs laser initiated recombination reactions, lateral interactions within the adsorbate layer become important for coverages $\theta > 0.5$ ML. Also, the work function was observed to increase with coverage up to ~0.5 ML hydrogen, but beyond 0.5 ML it decreases again.[21]

We conclude that the adsorbate−adsorbate interactions in the H/Ru(001) system originate from coverage-dependent changes in the electronic structure of the absorbate−substrate complex. Related effects are known in promotion and poisoning effects in heterogeneous catalysis due to coadsorption of other adsorbate species.[35] For small adsorbates such as hydrogen, steric repulsion between neighboring sites can be neglected and indirect, i.e., substrate-mediated interactions dominate.[36,37] For example, H-coverage dependent photoemission experiments from Ni and Pd reveal pronounced changes in the band structure of the metal substrate, even at low coverages.[38] Such changes in the electronic structure may also affect the electronic friction coefficient and hence the coupling time τ_{el} for energy flow into the adsorbate coordinate. Therefore, both a coverage dependent friction coefficient and changes in the adsorbate binding energy with coverage may contribute to the reported coverage dependence of the fs laser-induced desorption yield.

Conclusions

The prototypical photoreaction $H_{ad} + H_{ad} \rightarrow H_{2,gas}$ on Ru(001) initiated by intense near-infrared femtosecond laser excitation has been investigated, and results on the excitation mechanism, energy flow, and adsorbate−adsorbate interactions have been obtained. Two-pulse correlation measurements and the fluence dependence of the desorption yield and of the isotope effect reveal an ultrafast electron-mediated reaction pathway, in which electronic and nuclear degrees of freedom are nonadiabatically coupled. Multiple electronic transitions transfer energy from the photoexcited electronic subsystem into vibrational motion relevant for the associative desorption process. In addition, the high reaction efficiency is manifested in saturation effects in the reaction yield and in a large value for the reaction cross section obtained from decay curves in multiple-pulse experiments. The pronounced coverage dependence of the fs laser-induced yield above 0.5 ML is attributed to adsorbate−adsorbate interactions, which also play a role under thermal excitation conditions as seen in TPD data.

Recent studies on the dissociative adsorption of hydrogen on Pd, the time reversal of the associative desorption, further corroborate the importance of strong adsorbate−adsorbate interactions.[39] In this process not only both reactants (i.e., the two H atoms) but also the surrounding plays a crucial role. The dissociative adsorption of a H_2 molecule seems to require, contrary to conventional thinking, more than the necessary two-vacancy sites on the surface for an effective reaction. In our fs laser experiments with isotope-mixed layers on Ru, a dynamic promotion effect was observed, which also depends on the degree of excitation of the reactants' surrounding.[16] These cooperative effects in surface reactions are likely due to local changes of the electronic structure (and the potential energy landscape) of the reactants mediated by displacements of surrounding coadsorbates.

In adsorption experiments on thin metal films with Schottky contact, it was recently demonstrated, how crucially electron−hole pair excitations are coupled to nuclear motions and that these effects are not negligible even for low-energy processes for which phonon excitations are thought to dominate.[40,41] As a consequence, it was proposed that nonadiabatic electron−vibrational coupling routinely participate in reactions at metals, unlike in the traditional view, in which energy transfer occurs solely via phonons in the electronic ground state. By virtue of the highly nonequilibrium excitation conditions intrinsic to femtosecond laser experiments, the results reported here provide detailed insights that are of more general relevance for surface reaction dynamics.

Acknowledgment. We gratefully acknowledge contributions by Ch. Hess in the initial stage of the experiments. We thank the Deutsche Forschungsgemeinschaft for financial support through Sfb450.

References and Notes

(1) Eyring, H. *Chem. Phys.* **1935**, *3*, 786. Evans, M. G.; Polanyi, M. *Trans. Faraday Soc.* **1935**, *31*, 875.
(2) Greber, T. *Surf. Sci. Rep.* **1997**, *28*, 1.
(3) Nienhaus, H. *Surf. Sci. Rep.* **2002**, *45*, 1.
(4) Persson, B. N. J.; Persson, M. *Solid State Commun.* **1980**, *36*, 175.
(5) Diekenhöner, L.; Hornekar, L.; Mortensen, H.; Jensen, E.; Baurichter, A.; Petrunin, V. V.; Luntz, A. C. *J. Chem. Phys.* **2002**, *117*, 5018.
(6) Cavanagh, R. R.; King, D. S.; Stephenson, J. C.; Heinz, T. F. *J. Phys. Chem.* **1993**, *97*, 786.
(7) Lisowski, M.; Loukakos, P. A.; Bovensiepen, U.; Stähler, J.; Gahl, C.; Wolf, M. *Appl. Phys. A* **2004**, *78*, 165.
(8) Budde, F.; Heinz, T. F.; Loy, M. M. T.; Misewich, J. A.; de Rougemont, F.; Zacharias, H. *Phys. Rev. Lett.* **1991**, *66*, 3024. Misewich, J. A.; Kalamarides, A.; Heinz, T. F.; Höfer, U.; Loy, M. M. T. *J. Chem. Phys.* **1994**, *100*, 736.
(9) Kao, F.-J.; Bush, D. G.; Gomes da Costa, D.; Ho, W. *Phys. Rev. Lett.* **1993**, *70*, 4098. Her, T.-H.; Finlay, R. J.; Wu, C.; Mazur, E. *J. Chem. Phys.* **1998**, *108*, 8595. Bonn, M.; Funk, S.; Hess, C.; Denzler, D. N.; Stampfl, C.; Scheffler, M.; Wolf, M.; Ertl, G. *Science* **1999**, *285*, 1042.
(10) Brandbyge, M.; T.; Hedegard, P.; Heinz, T. F.; Misewich, J. A.; Newns, D. M. *Phys. Rev. B* **1995**, *52*, 6042.
(11) Misewich, J. A.; Heinz, T. F.; Newns, D. M. *Phys. Rev. Lett.* **1992**, *68*, 3737.
(12) *Handbook of Heterogeneous Catalysis*; Ertl, G., Knözinger, H., Weitkamp, J., Eds.; VCH: Weinheim, 1997.
(13) Van de Walle, C. G.; Neugebauer, J. *Nature* **2003**, *423*, 626.
(14) Christmann, K. *Prog. Surf. Sci.* **1995**, *48*, 15. Somorjai, G. A. *J. Phys. Chem. B* **2002**, *106*, 9201.
(15) Christmann, K. *Surf. Sci. Rep.* **1988**, *9*, 1.
(16) Denzler, D. N.; Frischkorn, C.; Hess, C.; Wolf, M.; Ertl, G. *Phys. Rev. Lett.* **2003**, *91*, 226102.
(17) Mate, C. M.; Somorjai, G. A. *Phys. Rev. B* **1986**, *34*, 7417. Astaldi, C.; Bianco, A.; Modesti, S.; Tosatti, E. *Phys. Rev. Lett.* **1992**, *68*, 90. Badescu, S.; Salo, P.; Ala-Nissila, T.; Ying, S. C.; Jacobi, K.; Wang, Y.; Bedürftig, K.; Ertl, G. *Phys. Rev. Lett.* **2002**, *88*, 136101.
(18) Funk, S.; Bonn, M.; Denzler, D. N.; Hess, Ch.; Wolf, M.; Ertl, G. *J. Chem. Phys.* **2000**, *112*, 9888.
(19) Feulner, P.; Menzel, D. *J. Vac. Sci. Technol.* **1980**, *17*, 662.
(20) Lindroos, M.; Pfnür, H.; Feulner, P.; Menzel, D. *Surf. Sci.* **1987**, *180*, 237.
(21) Feulner, P.; Menzel, D. *Surf. Sci.* **1985**, *154*, 465.
(22) Denzler, D. N.; Hess, C.; Funk, S.; Ertl, G.; Bonn, M.; Frischkorn, C.; Wolf, M. In *Femtochemistry and Femtobiology*; Douhal, A., Santamaria, J., Eds.; World Scientific: Singapore, 2002; p 652.
(23) Struck, L. M.; Richter, L. J.; Buntin, A.; Cavanagh, R. R.; Stephenson, J. C. *Phys. Rev. Lett.* **1996**, *77*, 4576.
(24) Budde, F.; Heinz, T. F.; Loy, M. M. T.; Misewich, J. A.; de Rougemont, F.; Zacharias, H. *Phys. Rev. Lett.* **1991**, *66*, 3024.

(25) Anisimov, S. I.; Kapeliovich, B. L.; Perel'man, T. L. *Sov. Phys. JETP* **1974**, *39*, 375.
(26) Budde, F.; Heinz, T. F.; Kalmarides, A.; Loy, M. M. T.; Misewich, J. A. *Surf. Sci.* **1993**, *283*, 143.
(27) Newns, D. M.; Heinz, T. F.; Misewich, J. A. *Prog. Theor. Phys.* **1991**, *106*, 411.
(28) Kao, F.-J.; Busch, D. G.; Cohen, D.; Gomes da Costa, D.; Ho, W. *Phys. Rev. Lett.* **1993**, *71*, 2094.
(29) Madey, T. E. *Science* **1986**, *234*, 316.
(30) Chou, M. Y.; Chelikowsky, J. R. *Phys. Rev. Lett.* **1987**, *59*, 1737.
(31) Feibelman, P. J.; Houston, J. E.; Davis, H. L.; O'Neill, D. G. *Surf. Sci.* **1994**, *302*, 81.
(32) Hoffmann, P.; Menzel, D. *Surf. Sci.* **1985**, *152*, 382.
(33) Lindroos, M.; Pfnür, H.; Menzel, D. *Surf. Sci.* **1987**, *192*, 421.
(34) Sokolowski, M.; Koch, T.; Pfnür, H. *Surf. Sci.* **1991**, *243*, 261.
(35) *The chemical physics of solid surfaces − Coadsorption, promoters and poisons*; King, D. A., Woodruff, D. P., Eds.; Elsevier: Amsterdam, 1993; Vol. 6.
(36) Bird, D. *Faraday Discuss.* **1998**, *110*, 335.
(37) Hammer, B.; Norskov, J. K. *Adv. Catal.* **2000**, *45*, 71.
(38) Greuter, R. G.; Strathy, I.; Plummer, E. W.; Eberhardt, W. *Phys. Rev. B* **1986**, *33*, 736.
(39) Mitsui, T.; Rose, M. K.; Fomin, E.; Ogletree, D. F.; Salmeron, M. *Nature* **2003**, *422*, 705.
(40) Gergen, B.; Nienhaus, H.; Weinberg, W. H.; McFarland, E. W. *Science* **2001**, *294*, 2521.
(41) Gadzuk, J. W. *J. Phys. Chem.* **2002**, *106*, 8265.